Heliyon 9 (2023) e20732

Contents lists available at ScienceDirect

Heliyon

journal homepage: www.cell.com/heliyon

Longitudinal association of epicardial and thoracic adipose tissues with coronary and cardiac characteristics in psoriasis

Ross O'Hagan [a,1], Li-Yueh Hsu [b,1], Haiou Li [a], Christin G. Hong [a], Philip M. Parel [a], Alexander R. Berg [a], Grigory A. Manyak [a], Vy Bui [b], Nidhi H. Patel [a], Elizabeth M. Florida [a], Heather L. Teague [a], Martin P. Playford [a], Wunan Zhou [a], Damini Dey [c], Marcus Y. Chen [a], Nehal N. Mehta [a], Alexander V. Sorokin [a,*]

[a] *Section of Inflammation and Cardiometabolic Diseases, National Heart, Lung, and Blood Institute, National Institutes of Health, Bethesda, MD, USA*
[b] *Radiology and Imaging Sciences, Clinical Center, National Institutes of Health, Bethesda, MD, USA*
[c] *Biomedical Imaging Research Institute, Cedars-Sinai Medical Center, Los Angeles, CA, USA*

ARTICLE INFO

Keywords:
Epicardial fat tissue
Prevention
Psoriasis
Computed tomography
Cardiovascular disease

ABSTRACT

Background: s: Psoriasis is a disease of systemic inflammation associated with increased cardiometabolic risk. Epicardial adipose tissue (EAT) and thoracic adipose tissue (TAT) are contributing factors for atherosclerosis and cardiac dysfunction. We strove to assess the longitudinal impact of the EAT and TAT on coronary and cardiac characteristics in psoriasis.
Methods: The study consisted of 301 patients with baseline coronary computed tomography angiography (CTA), of which 139 had four-year follow up scans. EAT and TAT volumes from non-contrast computed tomography scans were quantified by an automated segmentation framework. Coronary plaque characteristics and left ventricular (LV) mass were quantified by CTA.
Results: When stratified by baseline EAT and TAT volume quartiles, a stepwise significant increase in cardiometabolic parameters was observed. EAT and TAT volumes associated with fibro-fatty burden (FFB) (TAT: $\rho = 0.394$, $P < 0.001$; EAT: $\rho = 0.459$, $P < 0.001$) in adjusted models. Only EAT had a significant four-year time-dependent association with FFB in fully adjusted models ($\beta = 0.307$ $P = 0.003$), whereas only TAT volume associated with myocardial injury in fully adjusted models (TAT: OR = 1.57 95 % CI = (1.00–2.60); EAT: OR = 1.46 95 % CI = (0.91–2.45). Higher quartiles of EAT and TAT had increased LV mass and developed strong correlation (TAT: $\rho = 0.370$, $P < 0.001$; EAT: $\rho = 0.512$, $P < 0.001$).
Conclusions: Our study is the first to explore how both EAT and TAT volumes associate with increased cardiometabolic risk profile in an inflamed psoriasis cohorts and highlight the need for further studies on its use as a potential prognostic tool for high-risk coronary plaques and cardiac dysfunction.

Abbreviations: EAT, epicardial adipose tissue; TAT, thoracic adipose tissue; CCTA, coronary computed tomography angiography; CTA, computed tomography angiography; LV, left ventricular; NCB, non-calcified coronary burden; FFB, fibro-fatty burden; CVD, cardiovascular disease; PASI, psoriasis area and severity index; TC, total cholesterol; HDL-C, high-density lipoprotein-cholesterol; TG, triglycerides; ApoA1, apolipoprotein-A1; ApoB, apolipoprotein-B; hsCRP, high-sensitivity C-reactive protein; GlycA, glycoprotein acetylation; CAC, coronary artery calcium; IL-18, interleukin-18; IL-6, interleukin-6; TNF-α, tumor necrosis factor-α; MCP-1, *monocyte chemoattractant protein-1*.

* Corresponding author. Section of Inflammation and Cardiometabolic Diseases, National Heart, Lung and Blood Institute, Clinical Research Center, 9000 Rockville Pike, Bldg 10, Room 5-5150, Bethesda, MD, 20892, USA.
E-mail address: alexander.sorokin2@nih.gov (A.V. Sorokin).
[1] These authors contributed equally.

https://doi.org/10.1016/j.heliyon.2023.e20732
Received 19 July 2023; Received in revised form 3 October 2023; Accepted 5 October 2023

1. Introduction

Psoriasis is a disease of systemic inflammation associated with high rates of cardiometabolic complications and increased atherosclerosis [1,2]. Central to the atherogenic pathology is the uncontrolled inflammation associated with psoriatic skin disease that is driven, in part, by the secretion of cytokines accountable for the formation and rupture of atherosclerotic plaque. Indeed, epicardial adipose tissue (EAT), as depicted by computed tomography (CT), is a source of inflammatory cytokines that confers an increased risk of myocardial injury and has increased prevalence in psoriasis [3]. Although the exact mechanism is yet to be fully elucidated, current literature supports this portrayal of EAT as a pro-atherogenic mediator that may render plaque vulnerability [4]. Prior studies have demonstrated the association between high levels of EAT and incident cardiovascular disease (CVD) and mortality, as well as the relationship between increasing EAT and high-risk plaque features [5,6]. Of particular interest is the correlation between increased EAT volume and abnormal myocardial electric activity, suggesting the ability for EAT to disrupt the local architecture and cause myocardial injury [7]. Moreover, this relationship is further deteriorated by pro-inflammatory thoracic adipose tissue (TAT), which has also been shown to associate with coronary atherosclerosis [8] and increased CVD risk [9].

A growing body of evidence implicates EAT and TAT volumes with CVD, and there is a considerable interest at the prospect of utilizing these fat depots for CVD risk stratification in conditions with immunomodulated inflammatory mechanisms. Recent studies show that EAT volume is a valuable prognostic tool for early CVD risk assessment, including patients with psoriasis, and demonstrates the predictive capacity of EAT in heart failure outcomes [3,10]. These studies, however, have been limited in both sample size [3] and that the impact of EAT volume assessed by CT on either coronary characteristics or myocardial injury over time in psoriasis is yet to be assessed. Additionally, to the best of our knowledge, no study has shown the longitudinal impact of both EAT and TAT volumes on coronary plaque phenotypical changes. Therefore, this study sought to evaluate EAT and TAT volumes in psoriasis using an artificial intelligence-based CT image analysis with the following specific aims [1]: determine the clinical characteristics of those with increasing EAT and TAT volumes [2]; elucidate the association of EAT and TAT volumes with coronary artery characteristics, such as total coronary plaque burden, non-calcified coronary plaque burden and fibro-fatty plaque burden (TB, NCB, FFB), at baseline and over four years; and [3] explore the relationship between EAT and TAT volumes with early signs of myocardial damage, measured via left ventricular mass (LV mass) and troponin levels.

2. Materials and methods

2.1. Study participants

A collective 301 consecutive subjects with psoriasis were observed as part of an ongoing longitudinal cohort study from January 1, 2013 to July 12, 2022 (Psoriasis, Atherosclerosis, and Cardiometabolic Disease Initiative (NCT01778569) (Fig. 1). Patients were aged 18 years or older and had blood samples collected and coronary computed tomography angiography (CCTA) imaging performed at baseline, one year, and four years. All patients had a formal diagnosis of plaque psoriasis from a certified dermatologist. A certified healthcare provider assessed the patients Psoriasis Area Severity Index (PASI) score by gauging the onset, duration, and severity of skin disease. Patients were excluded if they had severe renal disease determined by an estimated glomerular filtration rate of less than 30

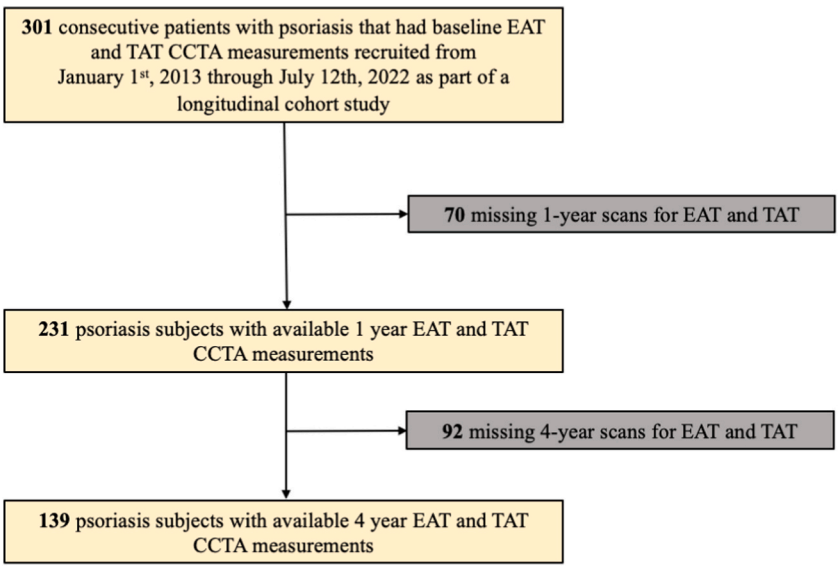

Fig. 1. Recruitment and follow-up scheme of study participants
CCTA, coronary computed tomography angiography; EAT, epicardial adipose tissue; TAT, thoracic adipose tissue.

mL/min/1.73 m^2 or were pregnant. The full details of the inclusion and exclusion criteria can be found on ClinicalTrials.gov. The study protocol was approved by the institutional review board of the National Institutes of Health and complied with the Declaration of Helsinki.

2.2. Clinical and biochemical measurements

Participants underwent measurements of routine vital signs, including waist circumference, and gave detailed histories. The specific psoriasis treatment at baseline was self-reported and included the following modalities: systemic therapy, biologic therapy, statins, light therapy, and topical treatments. Biologic therapy consisted of IL-17, TNF-α and IL-12/23 inhibitors.

Blood was collected for traditional plasma lipid parameters including total cholesterol (TC), high-density lipoprotein cholesterol (HDL-C), triglycerides (TG), as well as Apolipoprotein A-1 (ApoA-I), Apolipoprotein B (ApoB), high-sensitivity C-reactive protein (hsCRP) concentrations which were measured using commercially available enzymatic methods on the Cobas 6000 analyzer (Roche Diagnostics, IN, USA). LDL-C was calculated by the Friedewald equation. Glycoprotein acetylation (GlycA), a measure of systemic inflammation was assessed using the Vantera clinical NMR analyzer (Labcorp, NC, USA). Circulating high-sensitivity cardiac troponin-T (hs-cTn-T) was measured blindly with an immunoassay (Roche, Gen 5 STAT, Switzerland). hs-cTn-T value $>$ 6 ng/L, the lower limit of detection for this assay, was considered positive. Plasma cytokines quantities were calculated via multiplex enzyme-linked immunosorbent assay (ELISA) (Meso Scale Discovery, MD, USA). Other plasma biochemical measurements were performed on a Cobas 6000 analyzer in the NIH Clinical Center (Bethesda, MD, USA).

2.3. Coronary burden phenotype and cardiac characteristics by CTA

All participants underwent CCTA in the same scanner (320-detector row Aquilion ONE ViSION). Guidelines established by the NIH Radiation Exposure Committee were followed. Coronary artery characteristics across the main coronary arteries greater than 2 mm were phenotyped with QAngio CT (Medis, the Netherlands) which has a high intraclass correlation coefficient ($>$0.95) [11]. Only clear deviations of the software's semi-automatic contouring of lumen and outer wall segmentation were manually edited. Total, non-calcified and fibro-fatty coronary plaque burdens were calculated by dividing the respective coronary artery volume by corresponding segment length and were subsequently adjusted for mean lumen intensity determined via QAngio Ct. Fibro-fatty burden is defined as plaque with an accumulation of lipid-laden cells. Coronary artery calcium scoring (CAC) was evaluated by a cardiologist using semiautomated algorithms (SmartScore, GE Healthcare). CAC was measured via 40 continuous 3-mm thick computed tomographs (Imatron, CA, USA). Customized software (Imatron, CA, USA) was used by a radiological technologist to perform scoring. CAC scores underwent normalization via standard previously published methods [12].

2.4. Left ventricular mass measurement

A fully quantitative left ventricular (LV) mass quantification was performed using a fully automated software based on combined multi-atlas and corrective segmentation (CMACS) method for CCTA image segmentation as previously described [13–15]. The generated LV myocardium size was multiplied by a presumed myocardial tissue density of 1.05 g/mL. To standardize LV mass for varying heights and body mass indexes the mass was normalized to height to allometric power of 2.7 as previously discussed [16].

2.5. EAT and TAT volume characterization

EAT and TAT volumes were determined based on previously described methods in which CMACS framework for multi-structure segmentation of the heart and peripheral tissues from contrast enhanced CTA was used [14,15,17]. The CMACS framework was utilized to process both non-contrast and contrast-enhanced CTA image series and quantify EAT and TAT volumes in the inner thoracic cavity from the non-contrast image series. The framework first registers the non-contrast and contrast-enhanced series and then performs CMACS on the contrast-enhanced series. Next, segmentation labels are transferred to the non-contrast series to depict different structures within the thoracic cavity. EAT is quantified by counting the pixels within the whole heart region, excluding cardiac chambers and great vessels, and in the Hounsfield Units range of [−190,-30]. TAT volume is measured from the thoracic pixel space not occupied by both cardiac and non-cardiac tissue labels but includes EAT volume. The performance of the CMACS framework for EAT and TAT segmentation was validated by comparing our automated results with the results quantified from QFAT research software (version 2.0, Cedars-Sinai Medical Center, Los Angeles, CA) [18] based on 60 consecutive CTA scans of patients without coronary artery disease (CAD) [17].

2.6. Statistical analysis

Values were reported as mean (standard deviation [SD]) for parametric, median (interquartile range [IQR]) for nonparametric, and number (%) for categorical variables. Statistical significance was found through ANOVA for parametric variables, Kruskal-Wallis rank sum test for non-parametric variables, and Pearson chi-square test for categorical variables. Spearman correlation was applied for comparison between epicardial and thoracic adipose volumes and markers of interest at the baseline. Multivariable linear regression models were used to assess the relationship between EAT volume and coronary characteristics with possible risk factors adjustment. Confidence intervals were calculated via linear regressions. The relationship between fat factors with myocardial damage was

characterized based on logistic regression. A linear mixed-effect model was used to analyze the longitudinal impact of EAT and TAT volume on coronary burden over time and allowed for possible random intercept and random slopes of Apoa1 across participants. Adjustments were made via baseline covariates as listed. The longitudinal effect was estimated by the coefficient of interactions between EAT, TAT and time since baseline and the model was chosen based on likelihood ratio test. The effect was estimated by the standardized coefficient. $P < 0.05$ was considered statistically significant, and all analyses were performed with StataIC (version 16, StataCorp, TX, USA) and R (version 4.0.5, Vienna, Austria).

3. Results

3.1. Characteristics of the study group stratified by TAT and EAT volumes

Of the 301 study participants with both TAT and EAT volumes, the mean age of the study cohort was 50 ± 12.8 years, 62.8 % were male, and the median Framingham risk score was 2.0 [0.5–5.6] (Supplemental Table 1). When stratified by both baseline TAT and EAT volumes quartiles, a stepwise increase was associated with a significantly higher rate of hypertension, hyperlipidemia, metabolic

Table 1
Characteristics of psoriasis cohort stratified by thoracic adipose tissue volume at the baseline.

Parameter	Quartile 1	Quartile 2	Quartile 3	Quartile 4	P-Value
Demographic and Clinical Characteristics	N = 76	N = 75	N = 75	N = 75	
Age, y	43 ± 13.7	49 ± 12.6	53 ± 11.8	54.7 ± 11.1	**<0.001**
Males, n (%)	31 (41)	41 (55)	56 (75)	61 (81)	**<0.001**
Current smoker, n (%)	12 (16)	6 (9)	4 (5)	6 (9)	0.17
Hypertension, n (%)	11 (15)	10 (13)	22 (29)	36 (48)	**<0.001**
Type 2 diabetes, n (%)	3 (4)	10 (13)	8 (11)	14 (19)	**0.041**
Hyperlipidemia, n (%)	20 (26)	21 (28)	38 (51)	34 (45)	**0.002**
Metabolic syndrome, n (%)	5 (7)	16 (21)	29 (39)	40 (53)	**<0.001**
PASI score	4.6 (2.6–7.7)	5.0 (2.3–9.8)	6.0 (3.2–9.4)	7.0 (3.6–11.5)	0.07
FRS	0.42 (0.10–1.50)	1.56 (0.46–3.80)	3.71 (1.68–7.49)	4.76 (1.68–10.18)	**<0.01**
Biologic treatment, n (%)	19 (25)	24 (32)	22 (29)	25 (33)	0.69
Statin Treatment, n (%)	4 (5)	17 (24)	25 (34)	27 (37)	**<0.001**
Body mass index, kg/m^2	24.4 (21.5–26.70	27.2 (24.7–30.3)	29.8 (26.2–33.7)	32.3 (28.3–35.9)	**<0.001**
Waist to hip ratio	0.89 (0.84–0.94)	0.94 (0.89–0.99)	0.98 (0.94–1.02)	1.00 (0.96–1.05)	**<0.001**
Visceral adipose tissue, cm^3	5.0 (0.3–8.4)	11.7 (8.9–16.4)	19.6 (14.5–23.7)	22.9 (19.6–30.6)	**<0.001**
HOMA-IR	1.50 (1.15–2.11)	2.32 (1.32–3.76)	3.16 (2.34–5.11)	4.73 (3.23–7.32)	**<0.001**
GlycA, μmol/L	370 (333–425)	388 (347–448)	408 (370–450)	415 (364–460)	**0.003**
hsCRP, mg/L	1.2 (0.6–2.4)	1.3 (0.8–2.5)	1.9 (1.0–3.6)	2.5 (0.8–5.5)	**0.003**
Troponin, ng/L	6.59 ± 1.58	6.65 ± 1.30	7.26 ± 2.04	8.30 ± 4.70	**<0.001**
Lipids Parameters					
Triglycerides, mg/dl	77 (62–103)	96 (68–140)	115 (93–165)	132 (93–193)	**<0.001**
LDL cholesterol, mg/dL	96 (82–128)	109 (87–129)	110 (80–134)	101 (76–128)	0.56
HDL cholesterol, mg/dL	63 (55–73)	53 (43–63)	49 (42–57)	48 (41–60)	**<0.001**
Apolipoprotein A1, mg/L	168 (144–198)	150 (134–172)	143 (130–155)	142 (130–160)	**<0.001**
Apolipoprotein B, mg/L	83 (73–103)	93 (82–108)	93 (78–110)	96 (85–112)	**0.013**
Cytokine Profile					
Interleukin-6, pg/mL	1.32 (0.79–2.04)	1.07 (0.65–1.83)	1.26 (0.77–2.33)	1.60 (0.94–2.86)	**0.03**
Interleukin-8, pg/mL	3.20 (2.58–3.75)	3.21 (2.31–4.42)	3.55 (2.78–4.79)	4.37 (3.11–5.28)	**0.003**
Interleukin-18, pg/mL	380.57 (303.83–479.75)	354.64 (275.27–510.02)	426.85 (376.95–563.35)	523.70 (390.36–655.56)	**<0.001**
TNF-α, pg/mL	1.18 (0.71–1.70)	1.32 (0.83–1.85)	1.65 (1.11–3.76)	1.98 (1.09–6.18)	**0.003**
MCP-1, pg/mL	60.80 (32.37–110.09)	61.70 (26.29–123.01)	72.88 (35.13–134.11)	87.37 (41.49–144.23)	0.16
CTA Characteristics					
Total coronary burden, mm^2 (x100)	1.02 ± 0.46	1.08 ± 0.42	1.30 ± 0.42	1.37 ± 0.57	**<0.001**
Non-calcified coronary burden, mm^2 (x100)	0.95 ± 0.42	1.03 ± 0.43	1.24 ± 0.41	1.31 ± 0.56	**<0.001**
Fibrous Burden (x100)	0.78 ± 0.34	0.82 ± 0.32	0.95 ± 0.30	0.96 ± 0.44	**<0.001**
Fibro-fatty Burden (x100)	0.10 ± 0.08	0.14 ± 0.11	0.20 ± 0.14	0.23 ± 0.15	**<0.001**
Necrotic Burden (x100)	0.04 ± 0.13	0.04 ± 0.06	0.08 ± 0.17	0.11 ± 0.17	**0.007**
CAC score	0 (0–0)	0 (0–24)	0 (0–39)	6 (0–152)	**0.004**
LV mass, g	23.30 (20.51–25.55)	24.59 (22.27–27.74)	26.05 (22.98–28.92)	27.81 (24.75–30.58)	**<0.001**

Values are reported as mean ± SD for parametric data, median (interquartile range) for nonparametric continuous data, and N (%) for categorical data. The coronary burden is presented as the average burden measured in the left anterior descending, left circumflex, and right coronary arteries multiplied by 100. Bolded P values are significant. PASI, psoriasis area severity index; FRS, Framingham risk score; HOMA-IR, Homeostatic model assessment for insulin resistance; GlycA, Glycoprotein A; hsCRP, high sensitivity C-reactive protein; TNF-α, tumor necrosis factor-α; MCP-1, monocyte chemoattractant protein-1; CAC, coronary artery calcium score; LV mass, left ventricular mass.

syndrome, Framingham risk score, waist-to-hip ratio, visceral adiposity, insulin resistance (HOMA-IR) and inflammation by both GlycA and hsCRP when comparing Q4 to Q1 (Tables 1 and 2). There was a significant stepwise increase with psoriasis area severity index and type 2 diabetes when stratifying by TAT volume but not by EAT volume (TAT: P = 0.041; EAT: P = 0.230) (Tables 1 and 2).

Both EAT and TAT volumes had significant associations with lipid parameters, including triglycerides (TAT: ρ = 0.405; EAT: ρ = 0.409, P < 0.001 for all), HDL-C (TAT: ρ = −0.350; EAT: ρ = −0.389, P < 0.001 for all), Apo-A1 (TAT: ρ = -0.296; EAT: ρ = −0.326, P < 0.001 for all) and ApoB (TAT: ρ = 0.171, P = 0.003; EAT: ρ = 0.159 P = 0.006). However, neither EAT nor TAT volumes had a significant relationship with LDL-C (TAT: ρ = −0.12, P = 0.835; EAT: ρ = 0.001, P = 0.991) (Supplemental Table 2).

Both TAT and EAT volumes had evident correlation with interleukin-18 (IL-18) (TAT: ρ = 0.304, P < 0.001; EAT: ρ = 0.262, P = 0.001), interleukin-6 (IL-6) (TAT: ρ = 0.015, P = 0.015; EAT: ρ = 0.169 P = 0.015), IL-8 (TAT: ρ = 0.232, P = 0.001; EAT: ρ = 0.168 P = 0.015), and tumor necrosis factor-α (TNF-α) (TAT: ρ = 0.251, P < 0.001; EAT: ρ = 0.188, P = 0.007). Neither TAT nor EAT volumes had a significant relationship with monocyte chemoattractant protein-1 (MCP-1) (TAT: ρ = 0.135, P = 0.052; EAT: ρ = 0.097, P = 0.165) (Supplemental Table 2).

3.2. Association between EAT and TAT and coronary plaque characteristics

There was a significant association between the baseline EAT and TAT volumes and non-calcified burden (NCB) in unadjusted

Table 2
Characteristics of psoriasis cohort stratified by epicardial adipose tissue volume at the baseline.

Parameter	Quartile 1	Quartile 2	Quartile 3	Quartile 4	P-Value
Demographic and Clinical Characteristics	N = 76	N = 75	N = 75	N = 75	
Age, y	44 ± 13.4	51 ± 12.8	52 ± 12.1	53.9 ± 10.7	**<0.001**
Males, n (%)	27 (36)	42 (56)	57 (76)	63 (84)	**<0.001**
Current smoker, n (%)	8 (11)	11 (15)	2 (3)	7 (10)	0.10
Hypertension, n (%)	9 (12)	15 (20)	21 (28)	34 (45)	**<0.001**
Type 2 diabetes, n (%)	5 (7)	8 (11)	9 (12)	13 (17)	**0.23**
Hyperlipidemia, n (%)	20 (26)	27 (36)	29 (39)	37 (49)	**0.034**
Metabolic syndrome, n (%)	6 (8)	14 (19)	30 (40)	40 (53)	**<0.001**
PASI score	4.8 (2.6–7.5)	4.8 (2.8–9.0)	5.8 (2.8–9.7)	7.5 (4.3–11.8)	**0.015**
FRS	0.42 (0.14–1.4)	1.94 (0.42–4.7)	3.50 (1.40–6.10)	4.89 (1.88–11.00)	**<0.001**
Biologic treatment, n (%)	22 (29)	24 (32)	20 (27)	24 (32)	0.87
Statin Treatment, n (%)	6 (8)	20 (27)	19 (26)	28 (38)	**<0.001**
Body mass index, kg/m^2	23.3 (21.4–26.1)	27.1 (24.9–30.1)	29.8 (27.4–32.5)	32.9 (28.8–38.7)	**<0.001**
Waist to hip ratio	0.89 (0.84–0.93)	0.94 (0.88–0.98)	0.99 (0.93–1.02)	1.01 (0.97–1.05)	**<0.001**
Visceral adipose tissue, cm^3	4.6 (2.8–8.3)	11.6 (8.9–15.9)	18.6 (14.5–23.3)	23.9 (20.2–30.9)	**<0.001**
HOMA-IR	1.50 (1.15–2.15)	2.23 (1.41–4.03)	3.35 (2.32–5.06)	4.64 (3.05–7.04)	**<0.001**
GlycA, μmol/L	368 (332–401)	394 (350–449)	402 (362–445)	428 (374–464)	**<0.001**
hsCRP, mg/L	0.9 (0.5–2.1)	1.4 (0.9–3.1)	2.0 (0.7–3.3)	2.4 (1.0–5.0)	**<0.001**
Troponin, ng/L	6.33 ± 0.93	7.07 ± 1.85	7.27 ± 2.18	8.10 ± 4.54	**0.001**
Lipids Parameters					
Triglycerides, mg/dl	77 (61–106)	93 (66–131)	120 (91–167)	123 (97–193)	**<0.001**
LDL cholesterol, mg/dL	99 (82–127)	107 (84–134)	113 (84–133)	101 (78–128)	0.60
HDL cholesterol, mg/dL	64 (54–77)	55 (48–63)	48 (40–60)	47 (41–55)	**<0.001**
Apolipoprotein A1, mg/L	169 (142–202)	152 (137–169)	143 (126–161)	139 (130–153)	**<0.001**
Apolipoprotein B, mg/L	83 (73–103)	91 (78–105)	96 (86–110)	93 (81–112)	**0.004**
Cytokine Profile					
Interleukin-6, pg/mL	1.26 (0.72–2.11)	1.12 (0.69–1.95)	1.36 (0.77–2.30)	1.60 (0.91–2.89)	0.123
Interleukin-8, pg/mL	2.98 (2.58–3.75)	3.70 (2.21–4.84)	3.81 (2.81–5.05)	3.89 (2.92–4.95)	0.056
Interleukin-18, pg/mL	364.06 (300.43–472.95)	393.47 (305.42–581.35)	421.90 (362.69–550.54)	502.00 (353.94–611.29)	**0.001**
TNF-α, pg/mL	1.23 (0.69–1.98)	1.26 (0.94–2.12)	1.60 (1.12–3.51)	1.82 (1.02–4.86)	0.077
MCP-1, pg/mL	54.05 (23.18–84.92)	31.09 (29.90–130.01)	96.18 (40.60–141.21)	50.62 (32.58–85.11)	0.69
CTA Characteristics					
Total coronary burden, mm^2 (x100)	0.96 ± 0.30	1.11 ± 0.45	1.21 ± 0.46	1.49 ± 0.55	**<0.001**
Non-calcified coronary burden, mm^2 (x100)	0.90 ± 0.30	1.04 ± 0.41	1.16 ± 0.46	1.43 ± 0.54	**<0.001**
Fibrous Burden (x100)	0.73 ± 0.21	0.83 ± 0.33	0.88 ± 0.34	1.06 ± 0.45	**<0.001**
Fibro-fatty Burden (x100)	0.11 ± 0.08	0.14 ± 0.11	0.18 ± 0.12	0.25 ± 0.16	**<0.001**
Necrotic Burden (x100)	0.04 ± 0.12	0.04 ± 0.07	0.06 ± 0.12	0.12 ± 0.21	**0.003**
CAC score	0 (0–0)	0 (0–19)	4 (0–39)	3 (0–64)	**0.009**
LV mass g	22.50 (20.33–24.59)	25.03 (22.76–27.74)	26.10 (23.33–29.16)	28.39 (25.95–30.74)	**<0.001**

Values are reported as mean ± SD for parametric data, median (interquartile range) for nonparametric continuous data, and N (%) for categorical data. The coronary burden is presented as the average burden measured in the left anterior descending, left circumflex, and right coronary arteries multiplied by 100. Bolded P values are significant. PASI, psoriasis area severity index; FRS, Framingham risk score; HOMA-IR, Homeostatic model assessment for insulin resistance; GlycA, Glycoprotein A; hsCRP, high sensitivity C-reactive protein; TNF-α, tumor necrosis factor-α; MCP-1, monocyte chemoattractant protein-1; CAC, coronary artery calcium score; LV mass, left ventricular mass.

models (TAT: β = 0.290 P < 0.001; EAT: β = 0.329 P = 0.001) (Table 3). This relationship persists in a fully adjusted model factoring in age, sex, waist-to-hip ratio, statin use, and biologic treatment (TAT: β = 0.186 P = 0.006; EAT: β = 0.217 P = 0.001) (Table 3) (Fig. 2).

A similar baseline relationship was observed between both EAT and TAT volumes and fibro-fatty burden (FFB) in unadjusted models (TAT: β = 0.360 P < 0.001; EAT: β = 0.372 P = 0.001), and in a fully adjusted model (TAT: β = 0.259 P < 0.001; EAT: β = 0.253 P < 0.001) (Table 3) (Fig. 3).

Of the 301 study participants with baseline EAT and TAT volumes, 231 had EAT and TAT volumes at one year and 139 had EAT and TAT volumes at four years. For EAT volume, there was a significant relationship between NCB and EAT and also a significant interaction at four year in both unadjusted and fully adjusted models, indicating a time-dependent relationship between NCB and EAT (unadjusted EAT: β = 0.252 P = 0.002; fully adjusted EAT: β = 0.287 P < 0.001) (Table 4). For thoracic fat, the four-year interaction with NCB was insignificant but gained significance after adjustment (unadjusted TAT: β = 0.062 P = 0.416; fully adjusted TAT: β = 0.217 P = 0.004). For FFB, both EAT and TAT showed significant impact. On the other hand, there was a significant interaction between year four and EAT (unadjusted EAT: β = 0.297 P = 0.001; fully adjusted EAT: β = 0.307 P = 0.003) but not for TAT (unadjusted TAT: β = 0.143 P = 0.081; fully adjusted TAT: β = 0.131 P = 0.160) (Table 4).

3.3. Association between adipose tissue and cardiac characteristics

There was a significant association between baseline epicardial and thoracic adipose tissue and LV mass in unadjusted models (TAT: β = 0.353; EAT: β = 0.489 P < 0.001 for all). This relationship persisted when performing stepwise adjustments for age (TAT: β = 0.371; EAT: β = 0.512 P < 0.001 for all); age and sex (TAT: β = 0.313; EAT: β = 0.478 P < 0.001 for all); and age, sex, and waist-to-hip ratio (TAT: β = 0.261; EAT: β = 0.445 P < 0.001 for all). Even after adjusting for age, sex, waist-to-hip ratio, statin use, and biologic treatment, there was still significance between both adipose tissues and LV mass (TAT: β = 0.269; EAT: β = 0.446 P < 0.001 for all) (Table 3). A similar trend was seen when exploring the log of LV mass (Fig. 4).

Next, we assessed myocardial damage defined by plasma troponin levels above 6 ng/L. A significant association between both EAT and TAT volume were observed in unadjusted models (TAT: OR = 2.05 95 % CI = (1.44–3.03); EAT: OR = 2.12 95 % CI = (1.46–3.19). This relationship remained significant in fully adjusted models for TAT volume but not for EAT volume (TAT: OR = 1.57 95 % CI = (1.00–2.60); EAT: OR = 1.46 95 % CI = (0.91–2.45) (Table 5).

Of the 301 study participants, 196 had EAT and TAT volume and left ventricular (LV) mass at one year, 127 at four years. No significant time interaction was detected indicating that the fat factor effect persists at three time points. For EAT volume, a significant relationship with LV mass in both unadjusted and fully adjusted models was observed, indicating a time-dependent relationship between LV mass and EAT (unadjusted EAT: β = 0.364 P < 0.001; fully adjusted EAT: β = 0.283 P < 0.001). For thoracic fat, there was also a significant unadjusted and adjusted time dependent relationship with LV mass (unadjusted TAT: β = 0.283 P < 0.001; fully adjusted TAT: β = 0.293 P < 0.001).

3.4. Impact of biologic treatment initiation on adipose tissue

Finally, initiation of the psoriasis specific treatment in biologically naïve patients showed an increase in thoracic fat from baseline (99.8 cm^3 [52.7 cm^3–140.5 cm^3]) to 1 year (110.5 cm^3 [59.6 cm^3–166.4 cm^3]; P < 0.001). Conversely, biologic treatment showed a decrease in epicardial adipose tissue approaching statistical significance from baseline (52.9 cm^3 [27.8 cm^3–91.4 cm^3]) to 1 year (51.7 cm^3 (26.4 cm^3–89.9 cm^3]; P = 0.053) (Table 6).

Table 3
Regression analysis of coronary and cardiac characteristics at baseline.

	Epicardial Fat		Thoracic Fat	
	Standardized β	*P*-value	Standardized β	*P*-value
Non-calcified Burden				
Fat factor	0.329	**<0.001**	0.290	**0.001**
Fat factor + Age	0.387	**<0.001**	0.349	**<0.001**
Fat factor + Age + Sex	0.283	**<0.001**	0.239	**<0.001**
Fat factor + Age + Sex + WHR	0.202	**0.003**	0.173	**0.011**
Fat factor + Age + Sex + WHR + Statin Use + Biologic treatment	0.217	**0.001**	0.186	**0.006**
Fibro-fatty Burden				
Fat factor	0.372	**<0.001**	0.360	**<0.001**
Fat factor + Age	0.446	**<0.001**	0.439	**<0.001**
Fat factor + Age + Sex	0.341	**<0.001**	0.331	**<0.001**
Fat factor + Age + Sex + WHR	0.247	**<0.001**	0.252	**<0.001**
Fat factor + Age + Sex + WHR + Statin Use + Biologic treatment	0.253	**<0.001**	0.259	**<0.001**
Left Ventricular mass				
Fat factor	0.489	**<0.001**	0.353	**<0.001**
Fat factor + Age	0.513	**<0.001**	0.371	**<0.001**
Fat factor + Age + Sex	0.478	**<0.001**	0.313	**<0.001**
Fat factor + Age + Sex + WHR	0.445	**<0.001**	0.261	**<0.001**
Fat factor + Age + Sex + WHR + Statin Use + Biologic treatment	0.446	**<0.001**	0.269	**<0.001**

P-values ≤0.05 deemed significant (bolded values). Non-calcified burden and fibro-fatty burden were log transformed. WHR, Waist to hip ratio.

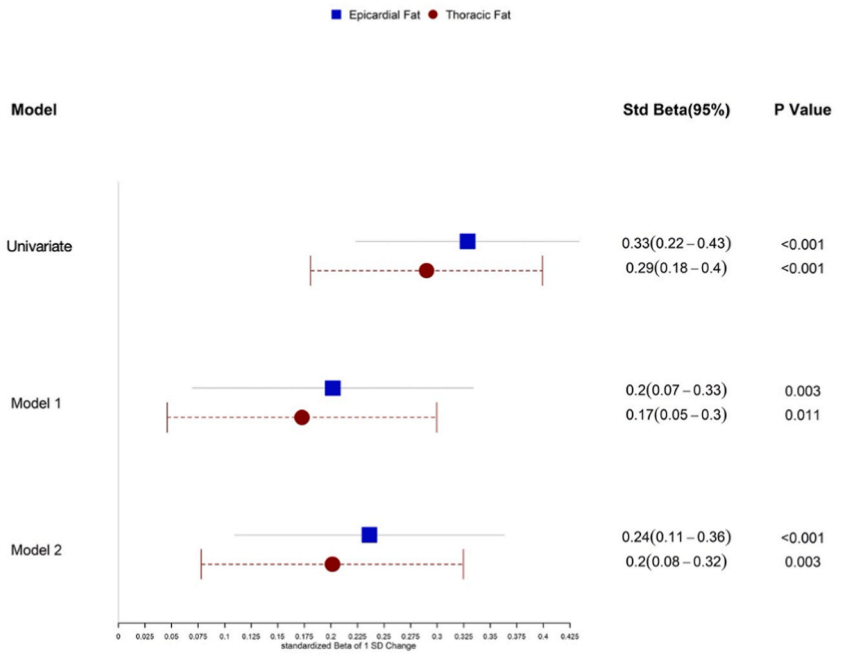

Fig. 2. Baseline epicardial and thoracic adipose volumes associate with non-calcified coronary burden in fully adjusted models
Log of non-calcified burden used for visualization purposes
Model 1: adjusted for age, sex, and waist-to-hip ratio
Model 2: adjusted for age, sex, waist-to-hip ratio, biologic treatment and statin therapy.

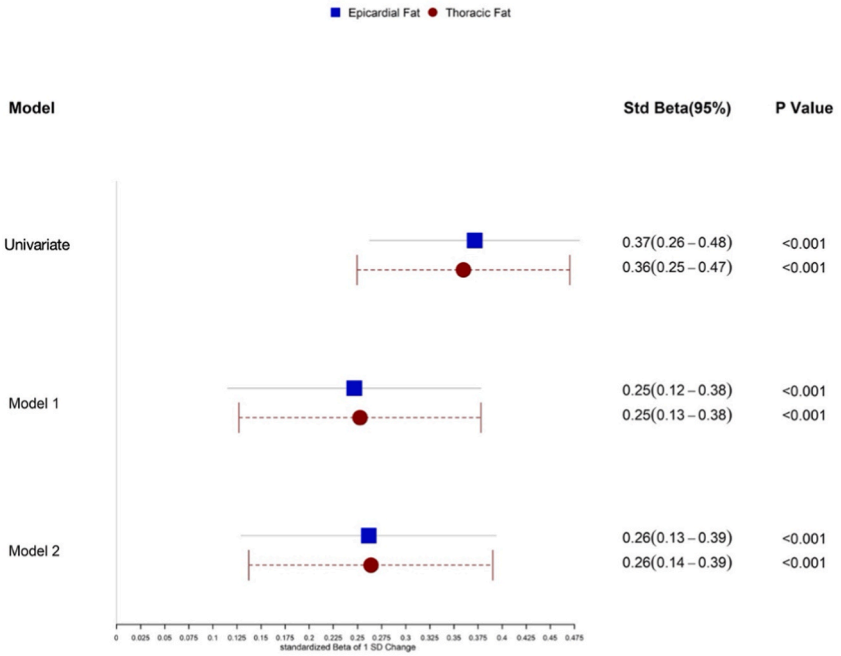

Fig. 3. Baseline epicardial and thoracic adipose volumes associates with fibro-fatty burden in fully adjusted models
Log of Fibro-fatty burden used for visualization purposes
Model 1: adjusted for age, sex, and waist-to-hip ratio
Model 2: adjusted for age, sex, waist-to-hip ratio, biologic treatment and statin therapy.

Table 4
Longitudinal analysis of coronary and cardiac characteristics.

	Epicardial Fat		Thoracic Fat	
	Standardized β	*P*-value	Standardized β	*P*-value
Non-calcified Burden				
Univariate Model				
Fat factor	**0.300**	**<0.001**	**0.262**	**0.001**
Fat factor * Year 1	**0.530**	**<0.001**	**0.429**	**<0.001**
Fat factor * Year 4	**0.252**	**0.002**	0.062	0.416
Model 1[1]				
Fat factor	**0.213**	**<0.001**	**0.187**	**<0.001**
Fat factor * Year 1	**0.437**	**<0.001**	**0.355**	**<0.001**
Fat factor * Year 4	**0.287**	**<0.001**	**0.217**	**0.004**
Fibro-fatty Burden				
Univariate Model				
Fat factor	**0.331**	**<0.001**	**0.318**	**<0.001**
Fat factor * Year 1	**0.540**	**<0.001**	**0.480**	**<0.001**
Fat factor * Year 4	**0.297**	**0.001**	0.143	0.081
Model 1[1]				
Fat factor	**0.260**	**<0.001**	**0.246**	**<0.001**
Fat factor * Year 1	**0.506**	**<0.001**	**0.446**	**<0.001**
Fat factor * Year 4	**0.307**	**0.003**	0.131	0.160
Left Ventricular mass				
Fat factor * Year 1	**0.364**	**<0.001**	**0.283**	**<0.001**
Fat factor * Year 1 + Model 1	**0.403**	**<0.001**	**0.293**	**<0.001**

P-values ≤0.05 deemed significant (bolded values).
Non-calcified burden and fibro-fatty burden were log transformed Model 1: adjusted for age, sex, waist-to-hip ratio, biologic and statin therapy.

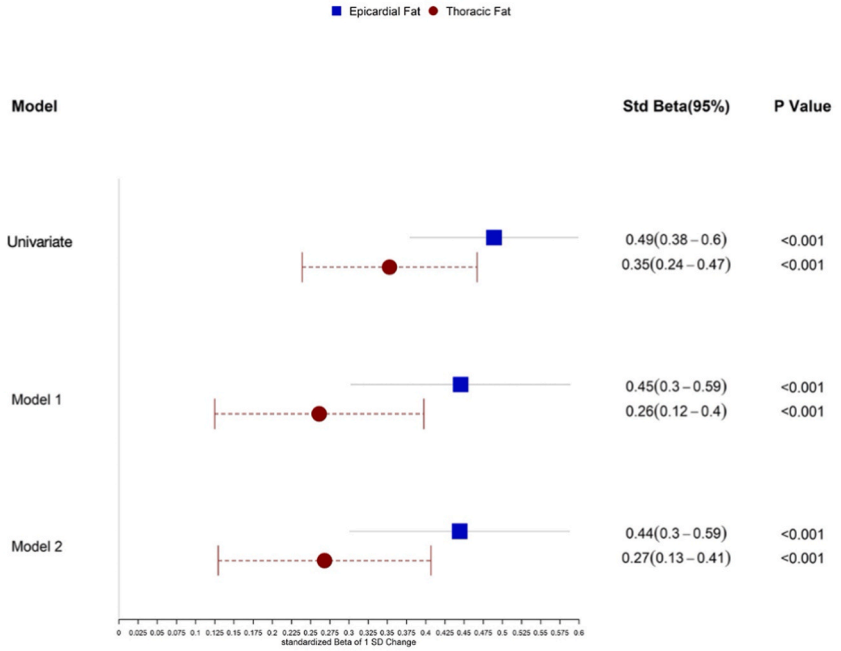

Fig. 4. Baseline epicardial and thoracic adipose volumes associates with left ventricular mass in fully adjusted models
Log of left ventricular mass used for visualization purposes
Model 1: adjusted for age, sex, and waist-to-hip ratio
Model 2: adjusted for age, sex, waist-to-hip ratio, biologic treatment and statin therapy.

4. Discussion

TAT and EAT are metabolically active tissues that secrete various proinflammatory cytokines and are linked to increased CVD risk [3](9). In this study, we explored characteristics of the psoriasis cohort stratified by both TAT and EAT volumes. Our study is unique in that most studies exploring the relation of EAT volume to coronary characteristics utilized transthoracic echocardiography, which is

Table 5
Regression analysis of binary troponin.

	Epicardial Fat		Thoracic Fat	
	Odds Ratio	95 % CI	Odds Ratio	95 % CI
Fat factor	**2.12**	**(1.46–3.19)**	**2.05**	**(1.44–3.03)**
Fat factor + Age	**1.81**	**(1.23–2.75)**	**1.73**	**(1.20–2.59)**
Fat factor + Age + Sex	1.27	(0.83–1.99)	1.34	(0.90–2.05)
Fat factor + Age + Sex + WHR	1.48	(0.91–2.46)	**1.56**	**(1.00–2.54)**
Fat factor + Age + Sex + WHR + Statin Use + Biologic treatment	1.46	(0.91–2.45)	**1.57**	**(1.00–2.60)**

P-values $\leq$0.05 deemed significant (bolded values). WHR, waist to hip ratio.

limited in assessing EAT volume [19]. However, our study used CT which has shown to be superior EAT volume quantification [19]. We found that those in the highest quartile of both TAT and EAT volumes had significantly higher rates of cardiometabolic pathologies such as hypertension, hyperlipidemia, and metabolic syndrome. These patients also had increased insulin resistance, inflammation, lipid abnormalities, and pro-inflammatory cytokine profile. Finally, there was increase in non-calcified burden, a marker of subclinical atherosclerosis; fibro-fatty burden, a marker of high rupture-prone plaque; left ventricular mass, an early sign of heart failure; and troponins, a marker of cardiac injury. We also found a significant relationship with markers of coronary and cardiac dysfunction in both fully adjusted baseline models and longitudinal models. Our findings suggest that both TAT and EAT volumes could be applied for early detection and risk assessment of CAD in patients with chronic inflammatory conditions, such as psoriasis.

While TAT and EAT volumes share some common biological properties, there were distinct differences observed. The highest percentile EAT group had an association with the psoriasis area severity index with absolute EAT values tended to decrease under specific biologic treatment over 1 year. Interestingly, TAT volumes did not have the same association and was following opposite change under the treatment. These discrepancies suggest that there might be some anatomical and biological factors related to protective function of either EAT or TAT, which needs further investigation. Of the explored inflammatory markers, the most had a statistically significant association with TAT than EAT volume. These markers besides hsCRP and GlycA also included pro-atherosclerotic cytokines, IL-6, IL-8, IL-18, TNF-α and MCP-1. Indeed, these cytokines reported to be involved in coronary plaque progression and rupture [20], as well as associated with increased risk for heart failure and myocardial infarction [21].

When we explored high-risk features of coronary atherosclerotic plaque, we found significant relationships between TAT and EAT volumes with NCB and FFB in fully adjusted baseline models. Additionally, fully adjustment revealed a time dependent longitudinal relationship between NCB and both TAT and EAT. However, there was only a significant time-dependent relationship between FFB and EAT. The observed difference might be in part explained by specific biological function of EAT over TAT, which besides unique cytokines profile also include matrix metalloproteinases (MMPs) release. Indeed, MMP-3 and MMP-9 are well known contributors to atherosclerotic plaque destabilization and subsequent rupture [22,23]. Moreover, EAT and TAT cellular composition and surrounded biologic environment might play a role as well. EAT is the only adipose tissue to have a direct connection to coronary arteries and has a distinct transcriptome from other adipose tissues [24–26]. EAT is known to have inflammatory impacts both systemically and locally in the coronary artery region [27]. It has even been shown the composition of EAT varies in those who are healthy and those with known CAD [28] highlighting complex relationship present with cardiac adipose and CAD.

Next, we assessed the relation of both TAT and EAT with cardiac function at baseline and 1 year. Cardiac function can be determined by left ventricular mass, which is linked to early heart failure and is driven by the inflammatory state in psoriasis [13]. We have previously demonstrated the relationship between inflammation and LV mass, which was mediated by non-calcified burden [13]. In the current study, we expanded these findings by showing an association between LV mass and both epicardial and thoracic adiposity. While prior work has shown a relationship between TAT [29] and EAT volumes [30] with the left ventricle mass, we confirmed its statistically significant association over time. Lastly, we observed the baseline relationship between the presence of troponin and epicardial and thoracic fat, which showed a strong relationship in unadjusted models. Of note, for fully adjusted models, there was only a significant relationship to TAT volume. EAT volume seems to have a more complex relationship to cytokines as EAT volume is known to release both cytokines with known protective and damaging cardiac complications [31]. This is potentially due to the EAT transcriptome containing cardioprotective adipokines such as adiponectin and adrenomedullin, which are known to have protective features against inflammation and atherosclerosis features [24,28,32]. Indeed, EAT volume is also known to have both protective features characteristic of white adipose and harmful features like brown adipose deeming it a "beige adipose" in adults [33]. The impact of EAT volume changing over time highlights the importance of exploring the systemic consequences of the changes in EAT composition. While it is possible TAT has cardioprotective features as well, these have not been supported strongly in the literature to the best of our knowledge.

Finally, there was a robust association between the visceral adipose tissue and measured EAT and TAT. Our group previously shown that active metabolic activity of visceral fat is associated with coronary plaque burden in psoriasis patients [34], as well represents a risk factor for developing CVD outcomes [35]. This observation may shed light on the potential connection between the visceral body fat and epicardial fat depots, which provides an exciting opportunity for improving CAD risk stratification in obese subjects.

While several studies have explored the relationship between TAT and EAT volumes, we are unique in showing the relationship between these adiposities and with both cardiac and coronary characteristics in a longitudinal manner. Our findings suggest that EAT volume may be better at monitoring heightened risk of rupture-prone fibro-fatty burden and TAT volume may be better at assessing baseline myocardial damage.

Table 6
Coronary plaque phenotype and cardiac characteristics change for biologic naïve patients treated over one year period.

Parameter CTA Characteristics	Baseline N = 66	One Year N = 66	P-value
Total coronary burden, mm^2 (x100)	1.24 ± 0.57	1.13 ± 0.51	**0.035**
Non-calcified coronary burden, mm^2 (x100)	1.19 ± 0.58	1.07 ± 0.51	**0.040**
Fibrous burden (x100)	0.88 ± 0.41	0.82 ± 0.34	**0.006**
Fibro-fatty burden (x100)	0.19 ± 0.17	0.20 ± 0.18	0.25
Necrotic burden (x100)	0.07 ± 0.14	0.05 ± 0.09	0.94
LV mass, g	26.72 ± 5.47	26.11 ± 5.61	0.94
Epicardial Fat, cm^3	52.88 (27.8–91.4)	51.7 (26.4–89.9)	0.053
Thoracic Fat, cm^3	99.8 (52.68–140.5)	110.5 (59.6–166.4)	**<0.001**
PASI score	9.0 (6.5–14.8)	2.4 (1.0–3.6)	**<0.001**

Values are reported as mean ± SD for parametric data, median (interquartile range) for nonparametric continuous data. The coronary burden is represented as average burden measured in the left anterior descending, left circumflex, and right coronary arteries multiplied by 100. Bolded P values are significant.
PACI, psoriasis area and severity index; LV mass, left ventricular mass.

In summary, we showed that individuals with increasing EAT and TAT volumes characterized by significantly higher associated cardiometabolic pathologies. There was a robust association between EAT and TAT with non-calcified and fibro-fatty coronary burdens at baseline. Over four years there was a significant relationship for EAT and TAT with non-calcified coronary burden in adjusted models. However, over four years there was only a significant relationship between EAT and fibro-fatty burden in adjusted models but not with TAT. We also found a significant relationship between TAT and myocardial damage assessed by troponin levels at baseline but not with EAT, whereas a significant relationship existed between both EAT and TAT with LV mass at one year in fully adjusted models.

Our study is limited by its prospective nature. Non-contrast imaging may have had some variations in kV and protocol between scans which is another limitation. The left ventricular mass was only standardized by one methodology when multiple exist, and we only had followed-up data in one year limiting the analysis of potential longer-term consequences. Additionally, the longitudinal cohort and the biologically naïve group were represented by a small number of observations, and we only explored the impact of time in one of many possible statistical methods. Another limitation was this algorithm was only explored in the psoriasis cohort so its generalized applicability to cohorts with systemic inflammation and CVD deserves further investigation.

In summary, our prospective study is the first to show the significant association between EAT and TAT volumes by CT and high-risk plaque in psoriasis over time. Thus, monitoring EAT and TAT volume in patients with psoriasis or any type of systemic inflammation may provide clinical utility. These findings substantiate the need for additional studies on the relationship between cardiac adiposities and lipoprotein metabolism dysfunction. TAT and EAT volumes may allow for noninvasive monitoring of patients at high risk for cardiovascular complications.

Ethics statement

Reviewed and approved by the Institutional Review Board of the National Institutes of Health (approval 13H-0065). Participants consented to having images published.

Data availability statement

Data will be made available on request.

CRediT authorship contribution statement

Ross O'Hagan: Conceptualization, Data curation, Formal analysis, Investigation, Methodology, Project administration, Supervision, Validation, Visualization, Writing – original draft, Writing – review & editing. **Li-Yueh Hsu:** Conceptualization, Formal analysis, Methodology, Validation, Visualization, Writing – original draft, Writing – review & editing. **Haiou Li:** Formal analysis, Methodology, Validation, Visualization. **Christin G. Hong:** Data curation, Formal analysis, Resources, Writing – review & editing. **Philip M. Parel:** Formal analysis, Methodology, Writing – original draft, Writing – review & editing. **Alex R. Berg:** Conceptualization, Formal analysis, Writing – review & editing. **Grigory A. Manyak:** Formal analysis. **Vy Bui:** Formal analysis. **Nidhi H. Patel:** Conceptualization, Investigation. **Elizabeth M. Florida:** Formal analysis. **Heather L. Teague:** Conceptualization, Formal analysis, Investigation, Methodology. **Martin P. Playford:** Data curation, Project administration, Resources. **Wunan Zhou:** Formal analysis, Writing – review & editing. **Damini Dey:** Conceptualization, Software. **Marcus Y. Chen:** Conceptualization, Investigation. **Nehal N. Mehta:** Conceptualization, Data curation, Formal analysis, Funding acquisition, Investigation, Methodology, Project administration, Writing – review & editing. **Alexander V. Sorokin:** Conceptualization, Data curation, Formal analysis, Funding acquisition, Investigation, Methodology, Project administration, Resources, Supervision, Validation, Visualization, Writing – original draft, Writing – review & editing.

Declaration of competing interest

The authors declare the following financial interests/personal relationships which may be considered as potential competing interests:Dr. Sorokin is a full-time US government employee.

Appendix A. Supplementary data

Supplementary data to this article can be found online at https://doi.org/10.1016/j.heliyon.2023.e20732.

References

[1] M. Aksentijevich, S.S. Lateef, P. Anzenberg, A.K. Dey, N.N. Mehta, Chronic inflammation, cardiometabolic diseases and effects of treatment: psoriasis as a human model, Trends Cardiovasc. Med. 30 (2020) 472–478.
[2] J.M. Gelfand, D.B. Shin, K.C. Duffin, et al., A randomized placebo-controlled trial of secukinumab on aortic vascular inflammation in moderate-to-severe plaque psoriasis (VIP-S), J. Invest. Dermatol. 140 (2020) 1784–1793.e2.
[3] C.N. Ellis, S.J. Neville, M. Sayyouh, et al., Epicardial adipose tissue volume is greater in men with severe psoriasis, implying an increased cardiovascular disease risk: a cross-sectional study, J. Am. Acad. Dermatol. 86 (2022) 535–543.
[4] A.M. Ansaldo, F. Montecucco, A. Sahebkar, F. Dallegri, F. Carbone, Epicardial adipose tissue and cardiovascular diseases, Int. J. Cardiol. 278 (2019) 254–260.
[5] N. Nerlekar, A.J. Brown, R.G. Muthalaly, et al., Association of epicardial adipose tissue and high-risk plaque characteristics: a systematic review and meta-analysis, J. Am. Heart Assoc. 6 (2017).
[6] R.H. Christensen, B.J. von Scholten, C.S. Hansen, et al., Epicardial adipose tissue predicts incident cardiovascular disease and mortality in patients with type 2 diabetes, Cardiovasc. Diabetol. 18 (2019) 114.
[7] C.J. Nalliah, J.R. Bell, A.J.A. Raaijmakers, et al., Epicardial adipose tissue accumulation confers atrial conduction abnormality, J. Am. Coll. Cardiol. 76 (2020) 1197–1211.
[8] P. Maurovich-Horvat, K. Kallianos, L.C. Engel, et al., Relationship of thoracic fat depots with coronary atherosclerosis and circulating inflammatory biomarkers, Obesity 23 (2015) 1178–1184.
[9] A.A. Mahabadi, T. Rassaf, Thoracic adipose tissue density as a novel marker of increased cardiovascular risk, Atherosclerosis 279 (2018) 91–92.
[10] V. Parisi, M. Conte, L. Petraglia, et al., Echocardiographic epicardial adipose tissue thickness for risk stratification of patients with heart failure, Front. Physiol. 11 (2020) 43.
[11] R. Symons, J.Z. Morris, C.O. Wu, A. Pourmorteza, M.A. Ahlman, J.A. Lima, M.Y. Chen, M. Mallek, V. Sandfort, D.A. Bluemke, Coronary CT angiography: variability of CT scanners and readers in measurement of plaque volume, Radiology 281 (3) (2016 Dec) 737–748.
[12] A.S. Agatston, W.R. Janowitz, F.J. Hildner, N.R. Zusmer, M. Viamonte Jr., R. Detrano, Quantification of coronary artery calcium using ultrafast computed tomography, J. Am. Coll. Cardiol. 15 (1990) 827–832.
[13] W. Zhou, M. Teklu, V. Bui, et al., The relationship between systemic inflammation and increased left ventricular mass is partly mediated by noncalcified coronary artery disease burden in psoriasis, Am J Prev. Cardiol 7 (2021), 100211.
[14] V. Bui, S.M. Shanbhag, O. Levine, et al., Simultaneous multi-structure segmentation of the heart and peripheral tissues in contrast enhanced cardiac computed tomography angiography, IEEE Access 8 (2020) 16187–16202.
[15] V. Bui, L.Y. Hsu, S.M. Shanbhag, et al., Improving multi-atlas cardiac structure segmentation of computed tomography angiography: a performance evaluation based on a heterogeneous dataset, Comput. Biol. Med. 125 (2020), 104019.
[16] C. Cuspidi, S. Meani, F. Negri, et al., Indexation of left ventricular mass to body surface area and height to allometric power of 2.7: is the difference limited to obese hypertensives? J. Hum. Hypertens. 23 (2009) 728–734.
[17] L. Hsu, V. Bui, R. O'Hagan, A. Sorokin, et al., Fully automated quantification of epicardial and thoracic adipose tissue from cardiovascular computed tomography, J. Cardiovas. Comput. Tomogr. 16 (2022) 3.
[18] D. Dey, Y. Suzuki, S. Suzuki, et al., Automated quantitation of pericardiac fat from noncontrast CT, Invest. Radiol. 43 (2008) 145–153.
[19] N. Nerlekar, Y.W. Baey, A.J. Brown, et al., Poor correlation, reproducibility, and agreement between volumetric versus linear epicardial adipose tissue measurement: a 3D computed tomography versus 2D echocardiography comparison, JACC Cardiovasc Imaging 11 (2018) 1035–1036.
[20] D.P. Ramji, T.S. Davies, Cytokines in atherosclerosis: key players in all stages of disease and promising therapeutic targets, Cytokine Growth Factor Rev. 26 (2015) 673–685.
[21] H.S. Sharma, D.K. Das, Role of cytokines in myocardial ischemia and reperfusion, Mediat. Inflamm. 6 (1997) 175–183.
[22] K. Magdalena, K. Magdalena, S. Grazyna, The role of matrix metalloproteinase-3 in the development of atherosclerosis and cardiovascular events, Ejifcc 17 (2006) 2–5.
[23] T. Li, X. Li, Y. Feng, G. Dong, Y. Wang, J. Yang, The role of matrix metalloproteinase-9 in atherosclerotic plaque instability, Mediat. Inflamm. 2020 (2020), 3872367.
[24] G. Iacobellis, Epicardial adipose tissue in contemporary cardiology, Nat. Rev. Cardiol. 19 (2022) 593–606.
[25] G. Iacobellis, D. Corradi, A.M. Sharma, Epicardial adipose tissue: anatomic, biomolecular and clinical relationships with the heart, Nat. Clin. Pract. Cardiovasc. Med. 2 (2005) 536–543.
[26] E.A. McAninch, T.L. Fonseca, R. Poggioli, et al., Epicardial adipose tissue has a unique transcriptome modified in severe coronary artery disease, Obesity 23 (2015) 1267–1278.
[27] G. Iacobellis, Local and systemic effects of the multifaceted epicardial adipose tissue depot, Nat. Rev. Endocrinol. 11 (2015) 363–371.
[28] G. Iacobellis, D. Pistilli, M. Gucciardo, et al., Adiponectin expression in human epicardial adipose tissue in vivo is lower in patients with coronary artery disease, Cytokine 29 (2005) 251–255.
[29] G. Iacobellis, M.C. Ribaudo, A. Zappaterreno, C.V. Iannucci, F. Leonetti, Relation between epicardial adipose tissue and left ventricular mass, Am. J. Cardiol. 94 (2004) 1084–1087.
[30] J.S. Kim, S.W. Kim, J.S. Lee, et al., Association of pericardial adipose tissue with left ventricular structure and function: a region-specific effect? Cardiovasc. Diabetol. 20 (2021) 26.
[31] E. Doukbi, A. Soghomonian, C. Sengenès, et al., Browning epicardial adipose tissue: friend or foe? Cells (2022) 11.
[32] G. Iacobellis, C.R. di Gioia, M. Di Vito, et al., Epicardial adipose tissue and intracoronary adrenomedullin levels in coronary artery disease, Horm. Metab. Res. 41 (2009) 855–860.
[33] H.S. Sacks, J.N. Fain, S.W. Bahouth, et al., Adult epicardial fat exhibits beige features, J. Clin. Endocrinol. Metab. 98 (2013) E1448–E1455.
[34] A. Sajja, K.M. Abdelrahman, A.S. Reddy, et al., Chronic inflammation in psoriasis promotes visceral adiposity associated with noncalcified coronary burden over time, JCI Insight 5 (2020).
[35] M. Teklu, W. Zhou, P. Kapoor, et al., Metabolic syndrome and its factors are associated with noncalcified coronary burden in psoriasis: an observational cohort study, J. Am. Acad. Dermatol. 84 (2021) 1329–1338.